



CHORUS

This is the accepted manuscript made available via CHORUS. The article has been published as:

Observation of fractional vortices and π phases in Josephson junctions involving periodic magnetic layers

I. P. Nevirkovets

Phys. Rev. B **108**, 024503 — Published 5 July 2023

DOI: [10.1103/PhysRevB.108.024503](https://doi.org/10.1103/PhysRevB.108.024503)

Observation of fractional vortices and π phases in Josephson junctions involving periodic magnetic layers

I. P. Nevirkovets

Department of Physics and Astronomy, Northwestern University, 2145 Sheridan Road, Evanston, Illinois 60208, USA

Abstract

Characteristics of $\text{SN}(\text{F}/\text{N})_n\text{IN}(\text{F}/\text{N})_m\text{S}$ Josephson junctions with $n, m = 1-3$ are reported; here S is a superconductor (Nb), F is a magnetic material (Ni), N is a non-magnetic metal (Al), and I is an insulator (Al/ AlO_x). The devices with $n = m = 1$ and $n = 1, m = 2$ display critical current vs magnetic field ($I_c(H)$) dependences which imply the appearance of fractional magnetic vortices in the junction, corresponding to a half of the flux quantum. Stochastic switching between the two half-vortex polarities with emission of an integer vortex was observed. In the devices with $n = m = 3$, a typical $I_c(H)$ dependence consists of a background current with a large modulation period, and a Fraunhofer-like pattern with a small modulation period on top of the background current. The Fraunhofer-like pattern may be completely or partially inverted; in these states, there is a component of the Josephson current flowing against the bias current, indicating the presence of the π phase in the junction. The experiments give evidence that switching between the 0 and π states can, potentially, be magnetically controlled.

1. Introduction

The two main advantages of superconducting electronics – high speed and low energy consumption – make it one of the candidates for beyond-CMOS future technologies [1-3]. Basic elements of the superconducting circuits are Josephson junctions made of two weakly connected superconductors [4,5]. In recent years, intense research is going on to integrate magnetic materials into Josephson junctions. Hybrid superconductor-ferromagnet (S/F) junctions reveal rich physics involving interplay between antagonistic order parameters, and offer the possibility of using the spin degree of freedom to control the superconducting state, thereby considerably expanding the functionality of existing devices and leading to the development of completely new capabilities for quantum information and sensing. Examples include: cryogenic memories [6-15], multi-terminal devices [16-18], Single-Flux Quantum (SFQ) circuits with improved performance [19], qubit

proposals [20,21], neuromorphic computing [22], etc.; see also recent reviews [23,24] and references therein.

SFQ circuits use an integer magnetic flux, $\Phi_0 = 2.07 \cdot 10^{-15}$ Wb, as the information carrier. This is based on a fundamental property of superconductors – flux quantization [25,26]. However, some superconducting systems can host fractional magnetic vortices containing the flux of $\Phi_0/2$. Two most known types of these systems are: (i) grain-boundary Josephson junctions based on superconductors with unconventional pairing symmetries, see review [27] and references therein, and (ii) $0 - \pi$ junctions [28,29] wherein one part of the junction is an ordinary SIS or SNS junction with the 0 phase difference in the ground state, and the second part contains a magnetic material in the barrier satisfying the condition of the π phase difference in the ground state.

Most research on S/F junctions has been carried out on devices involving 1–2 magnetic layers. A few works, focused on demonstration of spin-triplet supercurrents, reported devices involving three [30] or four [31] magnetic layers. In contrast to devices involving a few magnetic layers, periodic multilayered S/F systems may exhibit more complex behavior; however, experimental *phase-sensitive* research on S/F periodic multilayered systems is scarce.

Recently, a peculiar Josephson current, I_c , vs magnetic field, H , dependences were reported for hybrid $\text{SN}(\text{FN})_n\text{IN}(\text{FN})_m\text{S}$ and $\text{SN}(\text{FN})_n\text{S}$ junctions [32–34]; here, I denotes an insulator and N is a normal metal. In the devices [32–34], an averaged response of many F layers was observed. In this work, we introduce $\text{SN}(\text{FN})_n\text{IN}(\text{FN})_m\text{S}$ devices with n and m varied from 1 to 3. This new class of devices represents an intermediate case between the ordinary SIS junctions and the devices with many FN layers [32–34]. In the latter case, magnetic properties of the system are determined mainly by the average magnetization of all the layers. A distinctive feature of the devices considered here is that the magnetization of an individual F layer significantly influences the total magnetic profile leading to remarkable new effects reported below.

Specifically, in the lumped junctions with $n, m = 1$ and $n=1, m = 2$, we have observed magnetic interference patterns indicating the presence of fractional vortices containing the flux $\Phi_0/2$, and spontaneous switching between the opposite polarities of these vortices, similar to the instability predicted theoretically [35]. Furthermore, negative Josephson current and switching between the 0 and π phases is observed in the devices with $n, m = 3$. The observed physical properties may be useful for several applications in superconductive electronics.

2. Experimental

The multilayer $\text{SN}(\text{FN})_n\text{IN}(\text{FN})_m\text{S}$ structures (where S is Nb, F is Ni, N is Al, and I is AlO_x) were deposited onto oxidized Si substrates using DC magnetron sputtering of respective materials; the tunnel barrier was formed by thermal oxidation of the Al overlayer. The two-terminal junctions with lateral dimensions of $10\ \mu\text{m} \times 10\ \mu\text{m}$ were fabricated using the optical lithography, Reactive Ion Etching (RIE) of Nb in SF_6 plasma, Ar ion milling of the Ni/Al multilayers, anodization of the junction edges and the adjacent area of the bottom Nb electrode, and deposition of SiO_2 for insulation. The junctions were characterized in a liquid He bath at 4.2 K. The bias current through the junction was supplied perpendicular to the layers as shown schematically in Fig. 1(a). I - V curves and dependences of the maximum Josephson current, I_c , vs. external magnetic field, H , applied parallel to the structure plane, were measured.

3. Results

First, we consider characteristics of $\text{Nb}(120)\text{Al}(3.1)\text{Ni}(1.3)\text{Al}/\text{AlO}_x(3.1)\text{Al}(3.1)\text{Ni}(1.3)\text{Al}(3.1)\text{Nb}(70)$ junctions; here, the numbers in parentheses denote the thicknesses of the respective layers in nm. For $\text{Al}/\text{AlO}_x(3.1)$, the thickness is prior to oxidation. Fig. 1 shows $I_c(H)$ dependences of 6 nominally identical junctions; the field is presented in terms of the relative flux, Φ/Φ_0 . Here, Φ_0 is the flux quantum: $\Phi_0 = 2.07 \cdot 10^{-15}$ Wb. For the particular junction dimensions, the flux quantum corresponds to the magnetic field of about 11.1 Oe. In each measurement, the magnetic field was swept from “-” to “+” and backward. Therefore, each $I_c(H)$ curve consists of two branches which, in most cases, coincide with each other within the measurement error; no hysteresis is observed within the magnetic field range used in the experiment, except for one event described below. For five junctions, the measurement was repeated at least 2 times for each junction; one junction was measured only one time. Fig. 1 contains 15 dependences obtained on 6 junctions in all these measurements. The left inset in Fig. 1 shows initial portion of typical I - V curve of one of the junctions. Non-hysteretic property is an evidence that the junction is overdamped. The overall shape of the $I_c(H)$ dependences corresponds to that of the Fraunhofer-like pattern [36]. From the main panel, one can infer two main peculiar features characteristic of these junctions.

First, the $I_c(\Phi/\Phi_0)$ dependences are shifted along the Φ/Φ_0 axis from 0 by about $\pm 1/2$, i.e., the shift corresponds to a half-flux quantum, $\pm\Phi_0/2$. This is more clearly seen from the right-hand side inset in Fig. 1, which shows the top part of the main lobes of the $I_c(\Phi/\Phi_0)$ dependences on a magnified scale. The brackets' size equals to $\Phi/\Phi_0 = 1$. Therefore, the observed shift gives evidence of the formation of the half-flux-quantum vortices of the opposite polarities in the junctions, and the $I_c(\Phi/\Phi_0)$ dependence can be described by the relation

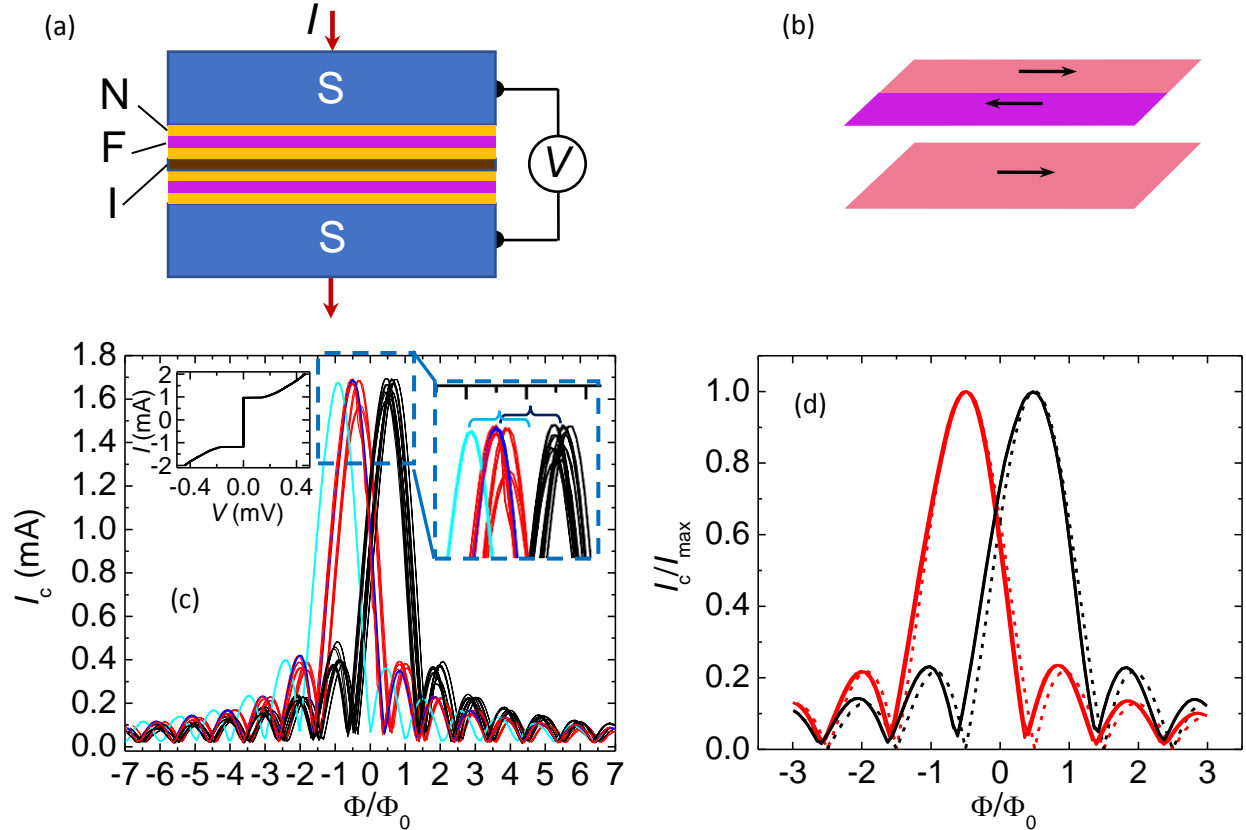


Fig. 1. (a) Schematic cross-sectional view of an SNFNINFNS Josephson junction and its biasing. Here, S is Nb, N is Al, F is Ni, and I is AlO_x . (b) Possible magnetization vectors configuration (denoted with arrows) of the two magnetic layers responsible for the fractional vortex appearance. (c) $I_c(\Phi)$ dependences recorded for 6 nominally identical SNFNINFNS junctions. All junctions display $\Phi_0/2$ shift of the Fraunhofer-like pattern; 4 junctions display stochastic behavior in the sense that repeating $I_c(H)$ measurement results in random switching of the Fraunhofer-like pattern between the $-\Phi_0/2$ and $+\Phi_0/2$ states (shown in red and black color, respectively). Right inset shows top portions of the main lobes on a magnified scale; bracket size equals to Φ_0 . Cyan curve shows Φ_0 shift for one of the junctions when sweeping the field from “-” to “+”. For the same junction, sweeping the field from “+” to “-” yields blue curve and the $-\Phi_0/2$ shift. Left inset shows initial portion of typical I - V curve of one of the junctions. (d) Solid black and red curves are experimental $I_c(H)$ dependences for one of the junctions. Dashed curves are theoretical dependences according to the relation $I_c = I_0 [\sin(\pi\Phi/\Phi_0 \pm \pi/2)] / (\pi\Phi/\Phi_0 \pm \pi/2)$.

$I_c = I_0[\sin(\pi\Phi/\Phi_0 \pm \pi/2)]/(\pi\Phi/\Phi_0 \pm \pi/2)$ shown in Fig. 1(d) by dashed curves along with the experimental dependence for one of the junctions (black and red solid curves for two measurement attempts). All six junctions displayed this behavior.

Second, a kind of stochastic behavior is observed: repeating the $I_c(H)$ measurement for the same junction randomly results in either negative or positive $\Phi_0/2$ shift, although positive shift tends to occur more frequently. This behavior was observed for 4 junctions. Two junctions (measured 1 and two times) displayed only $+\Phi_0/2$ shift. Only one junction displayed integer $-\Phi_0$ shift when the field was swept from “-” to “+”; see cyan curve in Fig. 1. For the same measurement attempt, when sweeping the field from “+” to “-”, the curve fell into the $-\Phi_0/2$ family (blue curve). In addition, one can notice a small “splitting” of the $-\Phi_0/2$ and $+\Phi_0/2$ $I_c(\Phi)$ states.

Similar behavior was observed for Nb(120)Al(3.1)Ni(1.3)Al/AIO_x(3.1)[Al(3.1)Ni(1.3)]₂Al(3.1)Nb(70) junctions. Total 6 nominally identical junctions of this type were measured. Two junctions, measured only one or two times, displayed usual Fraunhofer-like $I_c(H)$ dependence but with a $+\Phi_0/2$ shift. Four junctions, measured at least 2 times, displayed both $-\Phi_0/2$ and $+\Phi_0/2$ shifts.

Note that the behavior described above is drastically different from the shifts of the diffraction pattern for SIS’FS junctions reported in [6]. Those shifts, observed for the opposite directions of the magnetic field sweeping, were associated with the hysteresis of the magnetic moment, M , of the ferromagnetic material as a function of the externally applied magnetic field, and were not related with the flux quantum. In our case, within the field range used in the experiment, the $M(H)$ dependence is non-hysteretic (see, e.g., Fig. 2 in [33]), so that $I_c(H)$ branches for the two directions of H sweeping in most cases coincide with each other. The observed $\pm\Phi_0/2$ shifts reported in Fig. 1 are for the $I_c(H)$ curves involving *both* branches; the shifts occur randomly for identically repeated measurements.

In the case of Nb(120)[Al(3.1)Ni(1.3)]₂Al/AIO_x(3.1)[Al(3.1)Ni(1.3)]₂Al(3.1)Nb(70) junctions, the $\Phi_0/2$ shift was not observed; see $I_c(H)$ dependences for 7 nominally identical junctions of this type in Fig. 2. Instead, the background current and persistent oscillations at rather high applied magnetic fields are present in almost all junctions. Magenta, orange, and blue curves display signs of “negative” Josephson current with respect to the background current, i.e., for some values of the magnetic field, the lobes of the Fraunhofer-like pattern are inverted.

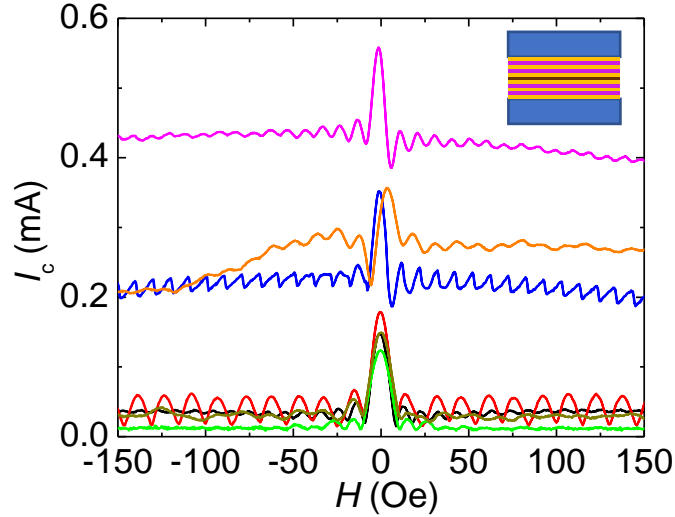


Fig. 2. $I_c(H)$ dependences recorded for 7 nominally identical Nb/[Al/Ni]₂/Al/AIO_x/[Al/Ni]₂Al/Nb junctions. Most of the junctions display background current and oscillations persistent at high magnetic fields. Magenta, orange, and blue curves display signs of “negative” Josephson current. Inset shows schematic of the structure.

The background current observed here and in the devices with many F layers [32-34] is also modulated by an applied magnetic field, but has a large modulation period. The nature of this current may be associated with the chiral edge currents characteristic of our multilayer junctions, and will be discussed in a more detail elsewhere [37]. In the junctions with many Ni/Al layers, the conductivity of the central part of the junction is poor [33,38], so that practically all supercurrent flows along the junction edges [33,36]. In the junctions with only a few Ni/Al layers, considered here, in addition to the edge supercurrents, some current flows also through the inner junction area; the latter results in an $I_c(H)$ dependence similar to that of an ordinary Josephson junction. This dependence is superposed on the background current associated with the mentioned edge currents. The interplay of the two supercurrents results in a reach variety of $I_c(H)$ shapes which we consider below for a specific case of Nb(115)[Al(3.1)Ni(1.3)]₃Al/AIO_x(3.1)[Al(3.1)Ni(1.3)]₃Al(3.1)Nb(68) junctions.

In these junctions, the abovementioned negative Josephson current is clearly manifested. A most pronounced case is shown in Fig. 3, where we plotted $I_c(H)$ dependences for a Nb/[Al/Ni]₃/Al/AIO_x/[Al/Ni]₃Al/Nb junction measured three times. Black curve was obtained in the first measurement; this type of curve was observed in about 50% cases (5 of 10 measured devices) and likely represents a most stable state in these junctions. However, this state can be changed under influence of the current through the junction, an externally applied magnetic field,

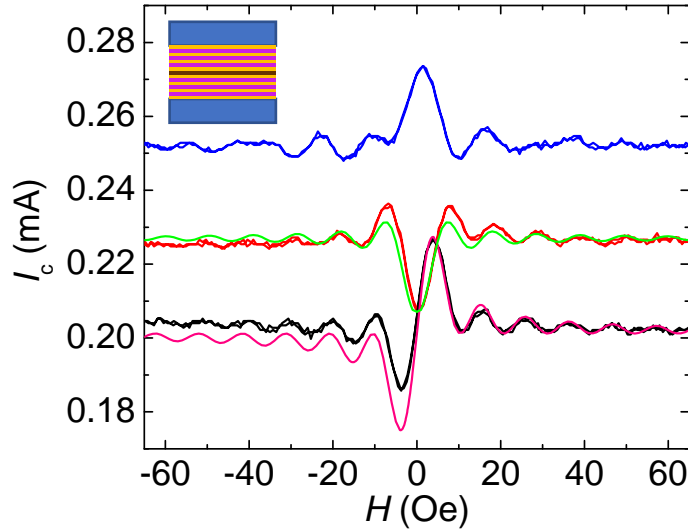


Fig. 3. $I_c(H)$ dependences for a Nb/[Al/Ni]₃/Al/AIO_x/[Al/Ni]₃Al/Nb junction measured three times. Black curve was obtained in the first measurement; blue curve was obtained after several consecutive measurements; and red curve was obtained after application of the field of about 350 Oe and thermal cycling. Green curve is theoretical dependence according to the relation $I_c = -I_0[\sin(\pi\Phi/\Phi_0)]/(\pi\Phi/\Phi_0)$ with $I_0 = 21 \mu\text{A}$ offset at 0.23 mA. Pink curve is theoretical dependence according to the relation $I_c = I_0[\sin^2(\pi\Phi/2\Phi_0)]/(\pi\Phi/2\Phi_0)$ with $I_0 = 26 \mu\text{A}$ offset at 0.21 mA. Φ_0 corresponds to 5.2 Oe. Inset shows schematic of the structure.

and some other factors not well understood at present, such as, e. g., switching between different magnetization configurations both within the same layer and across the multilayer. For example, blue curve in Fig. 3 was obtained after repeating the measurement several times; and red curve was obtained after further manipulations (application of the field of about 350 Oe and subsequent thermal cycling). The shape of the blue curve is similar to the standard Fraunhofer-like pattern superposed on top of a background current. The red curve represents an inverted Fraunhofer-like pattern, implying that a part of the Josephson current responsible for the pattern is flowing *opposite* to the main bias current. This dependence can be reasonably well fitted by the relation $I_c = -I_0[\sin(\pi\Phi/\Phi_0)]/(\pi\Phi/\Phi_0)$ with $I_0 = 21 \mu\text{A}$ and Φ_0 corresponding to 5.2 Oe (green curve in Fig. 3); the curve is offset at about 0.23 mA. Similar “negative” Josephson current was reported to occur in the disk-shaped 0- π junctions [39]. Our observation may be interpreted as competition between 0 and π phases in the multilayer SN(FN)_nIN(FN)_mS structures. Our experiment suggests that the type of the state, 0 or π , potentially, can be magnetically controlled. Indeed, according to the black curve in Fig. 3, for some magnetic state of the junction, “negative” Josephson current is present for the “negative” field, whereas turning the magnetic field to “positive” direction

switches the Josephson current to “positive”. To our knowledge, this kind of behavior was not reported yet for any kind of S/F junctions.

4. Discussion

Half-integer Josephson vortices, or semifluxons, are known to appear in $0-\pi$ junctions at the point where the Josephson phase experiences π discontinuity [35,39-42]. The discontinuity takes place on the length scale of the Josephson penetration depth, λ_J . Therefore, in order to host half-integer vortex, the minimum lateral size of the junction should be about λ_J . For our SNFNINFNS devices, the Josephson critical current density, j_c , is about $1.7 \cdot 10^7$ A/m². The effective magnetic thickness, d , can be evaluated as $d=2\lambda_L+t_{FN}+t_I$, where $\lambda_L=91$ nm is the London depth [33], and $t_{FN}+t_I=15$ nm is the total thickness of the Al, Ni, and AlO_x layers. Then $\lambda_J=(\hbar/2\mu_0ej_c d)^{-1/2}=8.9$ μm , i. e., λ_J is on the order of the junction size, 10 μm . Therefore, the occurrence of semifluxon is possible in such junctions. Although the mechanism of the formation of semifluxons in our junctions requires further study, one possibility of the formation of $0-\pi$ junction can be inferred from Fig. 1(b) where we show schematically a possible magnetization orientation in the two magnetic layers. Specifically, one of the F layers consists of two domains with the opposite magnetization, whereas the second layer has only one domain. In the part of the junction where the magnetizations of the domains are antiparallel (AP), the changes of the phase of the superconducting order parameter acquired in these domains completely (in the ballistic case) compensate each other [43-45]; in this part of the junction, the effective exchange field of the magnetic layers is negligible, and therefore, the respective region is supposed to be in the “0” state. On the other hand, in the part of the junction where the magnetizations of the domains are parallel (P), the phase changes add up, so that, if the total phase change is sufficient to make the order parameter negative, then this part of the junction is supposed to be in the “ π ” state. In this way, a $0-\pi$ junction can be obtained, necessary to create a semifluxon. Further research is needed to investigate if the proposed picture is indeed realized in our junctions.

Kuklov *et al.* [35] have shown theoretically that the external current is able to reorient the half-vortex by emitting an integer vortex to account for the total flux conservation. It appears that our observation of spontaneous switching of the $I_c(\Phi)$ dependence shown in Fig. 1 provides

evidence of similar process. Indeed, the two families of the $I_c(\Phi)$ curves are separated by the flux quantum, therefore, the junction randomly emits an integer vortex having opposite polarity for different switching events. We are not aware of a published work reporting such behavior.

Recently, significant attention of researchers is paid to the concept of a probabilistic or p-bit, a classical object whose state fluctuates between “0” and “1”, unlike a deterministic bit that is in “0” or “1” logic state at a given time [46-48]. Using appropriate superconducting elements with very low power consumption, such as Josephson junctions, would lead to very energy-efficient stochastic computing at low temperatures. Therefore, the development of p-bits based on Josephson junctions is highly desirable. Stochastic switching between the $-\Phi_0/2$ and $+\Phi_0/2$ states observed in our devices have potential for development of cryogenic p-bits.

Kirtley *et al.* [40] considered the spontaneous flux generation and magnetic field modulation of the critical current in a $0-\pi$ Josephson junction for different ratios of the junction length L to λ_J , and different ratios of the 0 -region length to the π -region length. In a particular case when the ratio of the lengths of the two regions is 1:1, the $I_c(\Phi)$ dependence is described with the relation $I_c=I_0[\sin^2(\pi\Phi/2\Phi_0)]/|(\pi\Phi/2\Phi_0)|$. In Fig. 3, we have fitted the black experimental curve with this dependence (omitting the modulus) by using Φ_0 corresponding to 5.2 Oe and $I_0=0.026$ mA (pink curve). The curve is offset at 0.21 mA from $I_c=0$ to account for the presence of the background current. The agreement between the theoretical and experimental curves is especially good for “positive” magnetic field, which implies that, likely, the SN[(FN)]₃IN[(FN)]₃S device involves 0 and π regions occupying approximately the same area.

Experimental observation and theoretical analysis of asymmetric $I_c(H)$ dependences for $0-\pi$ junctions was reported by Kemmler *et al.* [49]. The main non-ideal features of the experimental curves – a finite I_c value at minimum, asymmetric maxima, and a shift of the minimum along the field axis – were explained by the authors taking into account an asymmetry of the critical current density and different penetration of the magnetic flux in the 0 and π parts. The same factors may lead to a discrepancy between the black curve and the theoretical pink curve for “negative” field in our case (cf. Fig. 3).

Blue and red curves in Fig. 3 give evidence that 0 or π phases can occupy the entire region of the junction responsible for the Josephson current with a small oscillation period.

Remarkably, the presence of the background current allows to obtain a fully “inverted” Fraunhofer-like pattern (red experimental curve and the respective green theoretical curve).

5. Conclusion

We have fabricated and characterized at low temperatures multilayer $\text{SN}(\text{FN})_n\text{IN}(\text{FN})_m\text{S}$ devices with n, m from 1 to 3, where S is Nb, F is Ni, N is Al, and I is Al/ AlO_x . The devices described here displayed remarkable properties which, to our knowledge, were not reported in any type of Josephson junctions. The devices with $n = m = 1$ and $n = 1, m = 2$, in most cases, display regular-shape Fraunhofer-like critical current vs magnetic field dependences, but stochastically shifted along the H axis by a half of the period either to “negative” or “positive” fields. We interpret this behavior as the appearance of fractional magnetic vortices of the opposite polarities, corresponding to a half of the flux quantum; switching between the two polarities occurs by emitting an integer vortex. To our knowledge, such switching is observed for the first time. In the devices with $n = m = 3$, in most cases, the $I_c(H)$ dependence consists of a background current with very large modulation period, and a Fraunhofer-like pattern with a small modulation period on top of the background current. The Fraunhofer-like pattern may be completely or partially inverted; in these states, there is a component of the Josephson current flowing against the bias current, indicating the presence of the π phase in the junction. Our experiment gives evidence that switching between the 0 and π states is possible using the magnetic field. Currently, the physical picture of the processes taking place in the devices is not completely clear. It is obvious that the observed phenomena are related with the magnetic states of the F layers and their arrangement due to the mutual interaction and the interaction with the bias current and the applied magnetic field. Although at present full control of the behavior of the devices described here is not available, we believe that this will be possible in the optimized devices. The devices are promising for various applications in superconducting electronics, in particular, for stochastic computing. In order to implement these devices in practical circuits, better understanding of the underlying physics and control of the different states is necessary.

Acknowledgement

This research received support from NSF grant DMR 1905742 and from the NSF DISCoVER Expedition award under grant no. CCF- 2124453. The author acknowledges the use of facilities of the Materials Research Center at Northwestern University, supervised by J. B. Ketterson and supported by NSF. The author thanks M. A. Belogolovskii for fruitful discussions.

References

- [1] D. S. Holmes, A. L. Ripple, M. A. Manheimer, *IEEE Trans. Appl. Supercond.* **23**, 1701610 (2013).
- [2] I. I. Soloviev, N. V. Klenov, S. V. Bakurskiy, M. Yu. Kupriyanov, A. L. Gudkov, and A. S. Sidorenko, *Beilstein J. Nanotechnol.* **8**, 2689 (2017).
- [3] International Roadmap for Devices and Systems, <https://irds.ieee.org/home/what-is-beyond-cmos> (2018). Cheremhal
- [4] B. D. Josephson, *Phys. Lett.* **1**, 251 (1962).
- [5] K. K. Likharev, *Dynamics of Josephson junctions and circuits*, Gordon and Breach, NY, 1986.
- [6] I. V. Vernik, V. V. Bol'ginov, S. V. Bakurskiy, A. A. Golubov, M. Yu. Kupriyanov, V. V. Ryazanov, and O. A. Mukhanov, *IEEE Trans. Appl. Supercond.* **23**, 1701208 (2013).
- [7] B. Baek, W. H. Rippard, S. P. Benz, S. E. Russek and P. D. Dresselhaus, *Nature Commun.* **5**, 3888 (2014).
- [8] M. Abd El Qader, R. Singh, S. N. Galvin, L.Yu, J. Rowell, and N. Newman, *Appl. Phys. Lett.* **104**, 022602 (2014).
- [9] S. Mironov, E. Goldobin, D. Koelle, R. Kleiner, Ph. Tamarat, B. Lounis, and A. Buzdin, *Phys. Rev. B* **96**, 214515 (2017).
- [10] A. Murphy, D. V. Averin, and A. Bezryadin, *New J. Phys.* **19**, 063015 (2017).
- [11] I. P. Nevirkovets and O. M. Mukhanov, *Phys. Rev. Appl.* **10**, 034013 (2018).
- [12] G. E. Rowlands, C. A. Ryan, L. Ye, L. Rehm, D. Pinna, A. D. Kent, and T. A. Ohki, *Sci. Rep.* **9**, 803 (2019).
- [13] A. E. Madden, J. C. Willard, R. Loloee and N. O. Birge, *Supercond. Sci. Technol.* **32**, 015001 (2019).
- [14] R. de Andrés Prada, T. Golod, O. M. Kapran, E. A. Borodianskyi, Ch. Bernhard, and V. M. Krasnov, *Phys. Rev. B* **99**, 214510 (2019).
- [15] M.-H. Nguyen, G. J. Ribeill, M. V. Gustafsson, S. Shi, S. V. Aradhya, A. P. Wagner, L. M. Ranzani, L. Zhu, R. Baghdadi, B. Butters, E. Toomey, M. Colangelo, P. A. Truitt, A. Jafari-Salim, D. McAllister, D. IYohannes, S. R. Cheng, R. Lazarus, O. Mukhanov, K. K. Berggren, R. A. Buhrman, G. E. Rowlands, and T. A. Ohki, *Sci. Rep.* **10**, 248 (2020).
- [16] I. P. Nevirkovets, *Appl. Phys. Lett.* **95**, 052505 (2009).
- [17] I. P. Nevirkovets, O. Chernyashevskyy, G. V. Prokopenko, O. A. Mukhanov, and J. B. Ketterson, *IEEE Trans. Appl. Supercond.* **24**, 1800506 (2014).

- [18] I. P. Nevirkovets, O. Chernyashevskyy, G. V. Prokopenko, O. A. Mukhanov, and J. B. Ketterson, *IEEE Trans. Appl. Supercond.* **25**, 1800705 (2015).
- [19] N. K. Katam, O. A. Mukhanov, and M. Pedram, *IEEE Trans. Appl. Supercond.* **28**, 1300212 (2018).
- [20] T. Yamashita, K. Tanikawa, S. Takahashi, and S. Maekawa, *Phys. Rev. Lett.* **95**, 097001 (2005).
- [21] H. G. Ahmad, V. Brosco, A. Miano, L. Di Palma, M. Arzeo, D. Montemurro, P. Lucignano, G. P. Pepe, F. Tafuri, R. Fazio, and D. Massarotti, *Phys. Rev. B* **105**, 214522 (2022).
- [22] E. Jue, M. R. Pufall, I. W. Haygood, W. H. Rippard, and M. L. Schneider, *Appl. Phys. Lett.* **121**, 240501 (2022).
- [23] T. Yamashita, *IEICE Trans. Electron.*, **E104–C**, 422 (2021).
- [24] R. Cai, I. Žutic, and W. Han, *Adv. Quantum Technol.* 2200080 (2022).
- [25] B. Deaver and W. Fairbank, *Phys. Rev. Lett.* **7**, 43 (1961).
- [26] R. Doll and M. Näbauer, *Phys. Rev. Lett.* **7**, 51 (1961).
- [27] C. C. Tsuei and J. R. Kirtley, *Rev. Mod. Phys.* **72**, 969 (2000).
- [28] L. N. Bulaevskii, V. V. Kuzii and A. A. Sobyanin, *Solid State Commun.* **25**, 1053 (1978).
- [29] M. Weides, M. Kemmler, H. Kohlstedt, R. Waser, D. Koelle, R. Kleiner, and E. Goldobin, *Phys. Rev. Lett.* **97**, 247001 (2006).
- [30] J. W. A. Robinson, J. D. S. Witt, and M. G. Blamire, *Science* **329**, 59 (2010).
- [31] T. S. Khaire, M. A. Khasawneh, W. P. Pratt, Jr., and N. O. Birge, *Phys. Rev. Lett.* **104**, 137002 (2010).
- [32] I. P. Nevirkovets and O. M. Mukhanov, *Supercond. Sci. Technol.* **31**, 03LT01 (2018).
- [33] I. P. Nevirkovets, M. A. Belogolovskii, and J. B. Ketterson, *Phys. Rev. Appl.* **14**, 014092 (2020).
- [34] I. P. Nevirkovets, M. A. Belogolovskii, O. A. Mukhanov, and J. B. Ketterson, *IEEE Trans. Appl. Supercond.* **31**, 1800205 (2021).
- [35] A. B. Kuklov, V. S. Boyko, and J. Malinsky, *Phys. Rev. B* **51**, 11965 (1995).
- [36] K. K. Likharev, *Dynamics of Josephson junctions and circuits*, Gordon and Breach, NY, 1986.
- [37] M. A. Belogolovskii and I. P. Nevirkovets (unpublished).
- [38] A. Sharma, N. Theodoropoulou, T. Haillard, R. Acharyya, R. Loloee, W. P. Pratt, Jr., J. Bass, J. Zhang and M. A. Crimp, *Phys. Rev. B* **77**, 224438 (2008).
- [39] C. Gürlich, S. Scharinger, M. Weides, H. Kohlstedt, R. G. Mints, E. Goldobin, D. Koelle, and R. Kleiner, *Phys. Rev. B* **81**, 094502 (2010).
- [40] J. R. Kirtley, K. A. Moler, and D. J. Scalapino, *Phys. Rev. B* **56**, 886 (1997).
- [41] N. Lazarides, *Phys. Rev. B* **69**, 212501 (2004).
- [42] E. Goldobin, D. Koelle, and R. Kleiner, *Phys. Rev. B* **70**, 174519 (2004).
- [43] F. S. Bergeret, A. F. Volkov, and K. B. Efetov, *Phys. Rev. Lett.* **86**, 3140-3143 (2001).
- [44] Ya. M. Blanter and F. W. J. Hekking, *Phys. Rev. B* **69**, 024525 (2004).
- [45] J. W. A. Robinson, G. B. Halasz, A. I. Buzdin, and M. G. Blamire, *Phys. Rev. Lett.* **104**, 207001 (2010).

- [46] W. A. Borders, A. Z. Pervaiz, S. Fukami, K. Y. Camsari, H. Ohno and S. Datta, *Nature* **572**, 390-396 (2019).
- [47] K. Y. Camsari, B. M. Sutton, and S. Datta, *Appl. Phys. Rev.* **6**, 011305 (2019).
- [48] S. Ramanathan, J. Grollier, A. D. Kent, M. J. Rozenberg, I. K. Schuller, O. G. Shpyrko, R. C. Dynes, Y. Fainman, A. Frano, E. E. Fullerton, G. Galli, V. Lomakin, S. P. Ong, A. K. Petford-Long, J. A. Schuller, M. D. Stiles, Y. Takamura, and Y. Zhu, *APL Matter* **10**, 070904 (2022).
- [49] M. Kemmler, M. Weides, M. Weiler, M. Opel, S. T. B. Goennenwein, A. S. Vasenko, A. A. Golubov, H. Kohlstedt, D. Koelle, R. Kleiner, and E. Goldobin, *Phys. Rev. B* **81**, 054522 (2010).